SAND2008-1206C

# BENCHMARK ENCLOSURE FIRE SUPPRESSION EXPERIMENTS AND MODELING

Thomas K. Blanchat, Ph.D., Alexander L. Brown, Ph.D., and Victor Figueroa
Fire Science and Technology Department, Sandia National Laboratories
PO Box 5800 MS1135, Albuquerque, NM 87185
Voice: (505) 845-3048 email: tkblanc@sandia.gov

Sam S. Yoon, Ph.D.
Mechanical Engineering, Korea University
Anam-dong, 5-Ga, Sungbuk-gu, Seoul, 136-713, Korea

## ABSTRACT

This paper presents a series of benchmark fire suppression tests. The experiments were performed in a controlled environment utilizing a calorimeter centered above a 2 m diameter pan fueled with JP8. The experimental setup and procedure for gathering water suppression performance data are shown. Characteristics of the nozzles used in the testing are presented. The test results provide boundary and temporal data necessary for water spray suppression model development and validation. The paper also includes simulation results of the experimental work using a numerical model based on a temporally-filtered Navier-Stokes formulation using a Lagrangian approach for the droplets that includes detailed descriptions of the interaction between water droplets and fire plume. The test results concluded that the criterion for complete suppression depends on a combination factors to include nozzle diameter, nozzle operating condition, and presence of a calorimeter. The simulation results suggest the present adequacy of simulation tools for this application.

## INTRODUCTION

The objective of this work was to perform a series of new fire benchmark tests to provide required boundary and temporal data necessary for model development and validation. The tests would complement and expand historical water suppression data described in a literature review performed by Yoon [1]. The ultimate goal is to develop tools to assist the military services in the evaluation of high consequence asset response in an abnormal fuel fire environment. These tools include the simulation of fires that are started from spilled hydrocarbon fuel (e.g. JP-8). The benchmark experiments utilized JP-8 fuel and water spray suppression.

## EXPERIMENT SETUP AND PROCEDURE

The FLAME/Radiant Heat (FRH) test cell is part of the new Thermal Test Complex (TTC) at Sandia National Laboratories (SNL). Figure 1 shows the FRH facility with a pool fire at the ground level, pipes supplying air flow through the basement, the chimney, and instrumentation rooms outside the FRH chamber. The main test chamber of the FRH cell is cylindrical in shape (18.3 m inner diameter) with a height around the perimeter of 12.2 m. The ceiling slopes upwards (~18º) from the perimeter walls to a height of 14.6 m over the center of the facility. A round hole at the top of the facility (4.9 m diameter) transitions to a 3.0 m by 3.7 m chimney

duct. The outer walls are made of steel channel sections and are filled with water to maintain a relatively constant wall temperature during tests. The ground level of FRH can be divided into three concentric sections; a liquid fuel pan or gas burner (up to 3 m in diameter), spill plates, and grating for inlet combustion air. Typical liquid fuels include JP8, methanol, ethanol, and other hydrocarbons and typical gas fuels are hydrogen and methane. Air enters the FRH cell via the 3.05 m diameter pipe and is distributed by 18 supply pipes to an annulus along the subbasement circumference. Air entering the chamber ground level was characterized experimentally and shown to be uniform within 10% of the mean flow.

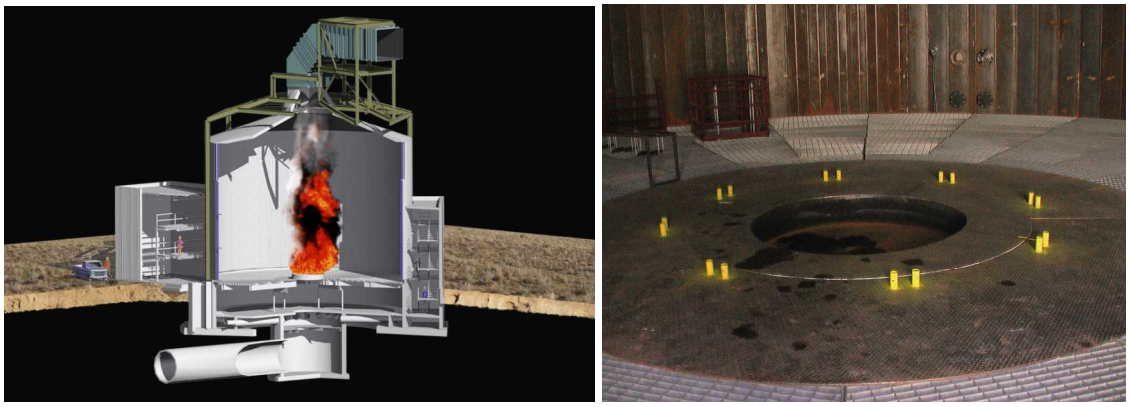

**Fig. 1. FLAME test cell and 2-m fuel pan.**

Figure 2 shows a test apparatus simulating a single-nozzle, water suppression system assembled inside FLAME. A 2-m long calorimeter was used is some experiments to determine the effects of the fire suppression with engulfed objects. The steel calorimeter was 0.3 m in diameter and was located approximately 0.7 m above the top of the pan. All tests were conducted using a 2 m diameter pan. A diesel-powered high pressure/high volume spray pump fed various nozzles via a nominal 1-1/2" diameter plumbing.

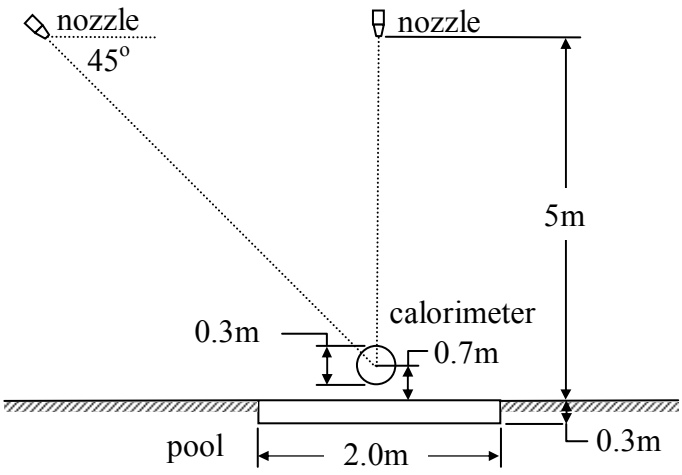


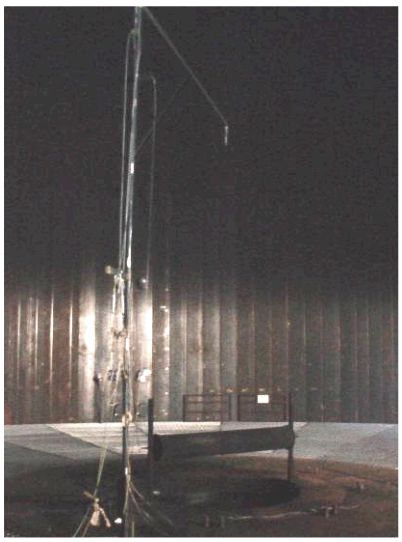

(a) (b)

**Fig. 2. Experiment setup and nozzle configurations.**

Two spray orientations (45° and 90°) were tested. In the 90° configuration the nozzle was positioned directly above the calorimeter and in the 45° configuration the nozzle was slightly less than 4.0 m from the center of the pan. In both configurations the nozzle was approximately 5 m from the top of the pan.

All nozzles (Table 1) used in these experiments were 30° full solid cone (Spraying Systems, Co., Wheaton, IL). This type of nozzle gives a uniform, round, full spray (as opposed to a hollow cone) pattern with medium-to-large droplet size. Pressure-flow rate characteristic curves were obtained. In addition, droplet information was obtained for nozzles 3014 (0.094") and 3050 (0.172"). A Phase Doppler Particle Analyzer (PDPA) was used to obtain droplet volume diameter and droplet velocity at 1 m from the exit of the nozzle and at three different locations along the diameter of the nozzle spray starting from the center (i.e., 0.0, 0.1 and 0.2 m).

**Table 1. Nozzle Data.**

| Nozzle Model No. | Nozzle Diameter (in) |
|---|---|
| 30200 | 0.344 |
| 30400 | 0.469 |
| 3014 | 0.094 |
| 3050 | 0.172 |

Figure 3 shows flow rate-pressure data (with curve fits) for all four nozzles in addition to the droplet volume mean diameters and velocities for the two characterized nozzles.

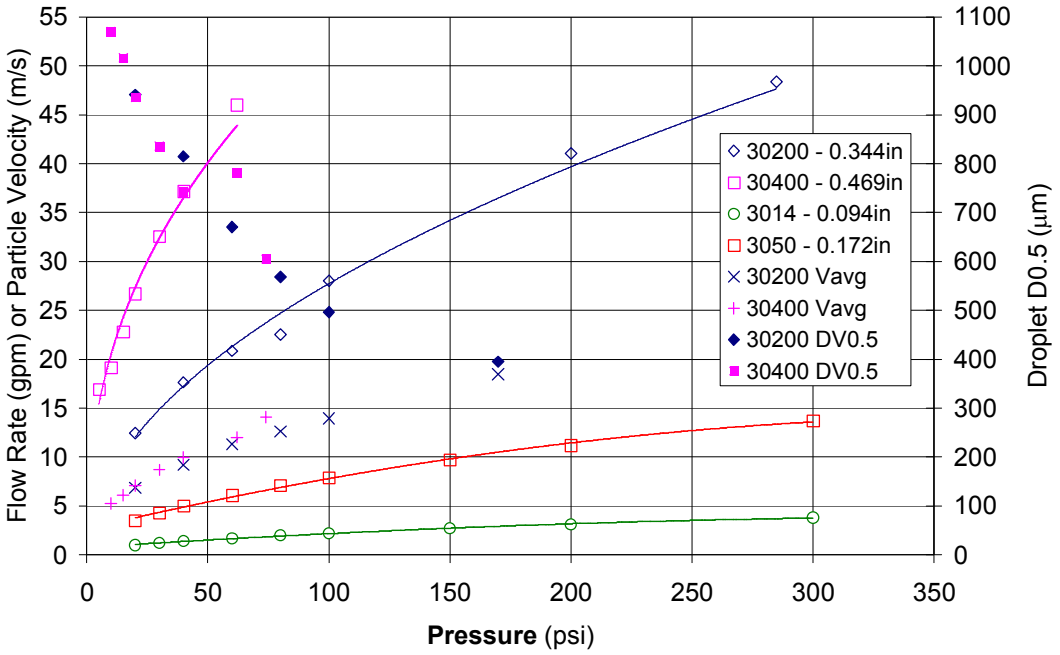


**Fig. 3. Nozzle flow rate, and droplet mean diameter and velocity as a function of pressure.**

The Volume Mean Diameter (VMD), D0.5, is a means of expressing droplet size in terms of the volume of liquid sprayed. The VMD is a value where 50% of the total volume (or mass) of liquid sprayed is made up of droplets with diameters larger than the mean value and 50% smaller than

the mean value. Note that the mean diameter decreases as the injection velocity increases. Since the turbulent Kolmogrov lengths scale decreases as the Weber number or Reynolds number decreases, the droplet size naturally reduces in response to the reduced dominant length scale.

Water line pressure was monitored upstream of the nozzle during each test. Four video cameras (in water-cooled enclosures) were placed at four different locations inside of FLAME. Two cameras recorded normal and parallel views of the fire; a third camera recorded the fire from above; a fourth camera monitored for spillage below the floor plane. A data acquisition system monitored nozzle water temperature and line pressure. For each test, the 2-m diameter pan was fueled using ~1.3 cm of JP-8 (poured on a water-layer), nominally providing about a 3 minute fire. The forced draft fan was energized and set to maintain an air flow rate of 150,000 scfm. After the fire was fully developed (1-2 minutes) the fire suppression system was activated. If the fire was extinguished, the suppression system was deactivated shortly thereafter. If the fire was not extinguished after about 30-40 seconds, the suppression system was turned off.

## SUPPRESSION TESTS RESULTS AND ANALYSIS

A total of 12 fire suppression benchmark test *cases* (48 total *experiments*) were conducted in the FLAME facility. The following parameters were varied in these tests: 1) the position of the spray injection (45° and 90° injection angle), 2) nozzle operating pressures, and 3) presence of the calorimeter. Tables 2 and 3 show test runs for 90° and 45° nozzle orientations, respectively. Two experiments were performed for each case, one with and one without a calorimeter. In addition, each experiment was repeated twice. Results showed that while the 90° test cases were repeatable, the 45° test cases were not in all cases.

**Table 2 Test Cases for 90° orientation.**

| Test No. | Operation Pressure (psi) | Flow Rate (gpm) | Nozzle Model No./ Diameter (in) |
|---|---|---|---|
| 1 | 52 | 42 | 30400/0.469 |
| 2 | 74 | 48 | 30400/0.469 |
| 3 | 190 | 39 | 30200/0.344 |
| 4 | 25 | 14 | 30200/0.344 |
| 5 | 100 | 28 | 30200/0.344 |
| 6 | 155 | 34 | 30200/0.344 |
| 7 | 317 | 4 | 3050/0.094 |
| 8 | 317 | 14 | 3014/0.172 |

**Table 3 Test Cases for 45° orientation.**

| Test No. | Operation Pressure (psi) | Flow Rate (gpm) | Nozzle Model No./ Diameter (in) |
|---|---|---|---|
| 1 | 25 | 14 | 30200/0.344 |
| 2 | 100 | 27 | 30200/0.344 |
| 3 | 155 | 34 | 30200/0.344 |
| 4 | 190 | 39 | 30200/0.344 |

Figure 4 shows the time series for the pool fire with nozzle 30200 injecting at 39 gpm with a calorimeter. The image taken at t=-0.333sec shows a typical fire prior to the spray injection. The image taken at t=0.000sec shows the fire structure when the water spray was initially injected. The suppression time is defined as the time at which the fire is not visible in the images. In reality the fire is extinguished near the fuel surface at a slightly earlier time even though flames remained visible in the upper region of the fire. In this case, the spray momentum was sufficiently high to reach the fuel surface; therefore, suppression (defined as a fully extinguished fire) was achieved with the calorimeter present (t=2.67±1/3 sec).

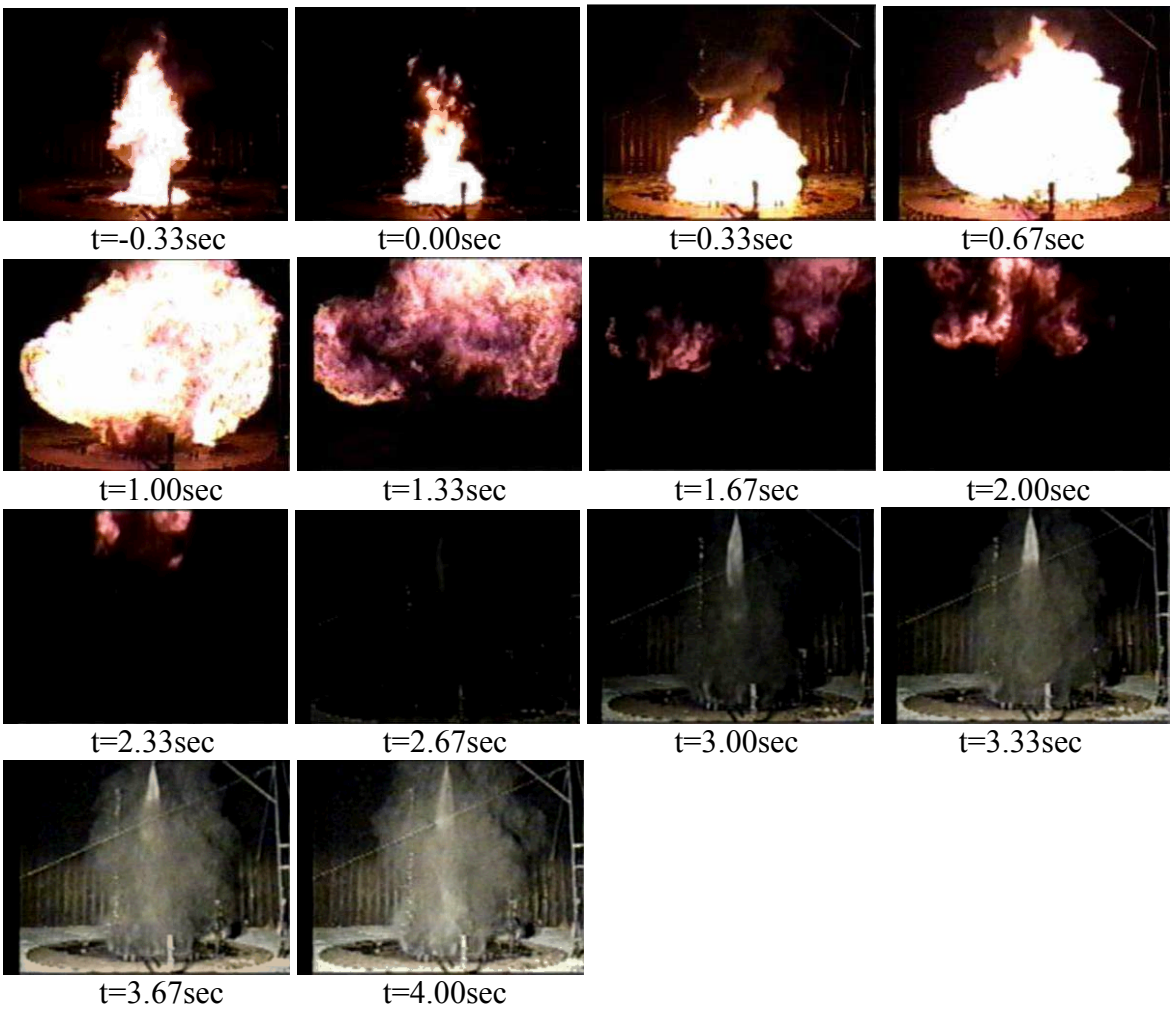


**Fig. 4. 90° Spray at 190 psi (39 gpm) *Without* the Calorimeter (Test 3).**

Notice that when the spray reached the flame, the fire intensity appears to increase, with a corresponding increase in the heat flux emitted to probes in the vicinity of the fire (see the images from t=0.33sec to t=1.33sec). This increase in fire intensity is believed to be caused by an enhanced fuel mixing rate.

Figure 5 summarizes results of suppression tests with the 90° nozzle configuration. The symbols in the figure point to the operating conditions of the test run. The labels "Supp" and "No Supp" in the figure indicate the operating conditions where suppression was achieved or not achieved, respectively, and is true whether the calorimeter was present or not. The label "Supp only for w/o calo" indicates suppression was achieved only for the case without the calorimeter. Based on experiment results for the cases without the calorimeter, a rough critical line was constructed. Any operating regime below the critical line did not yield a suppression condition and any operating regime above the line resulted in suppression.

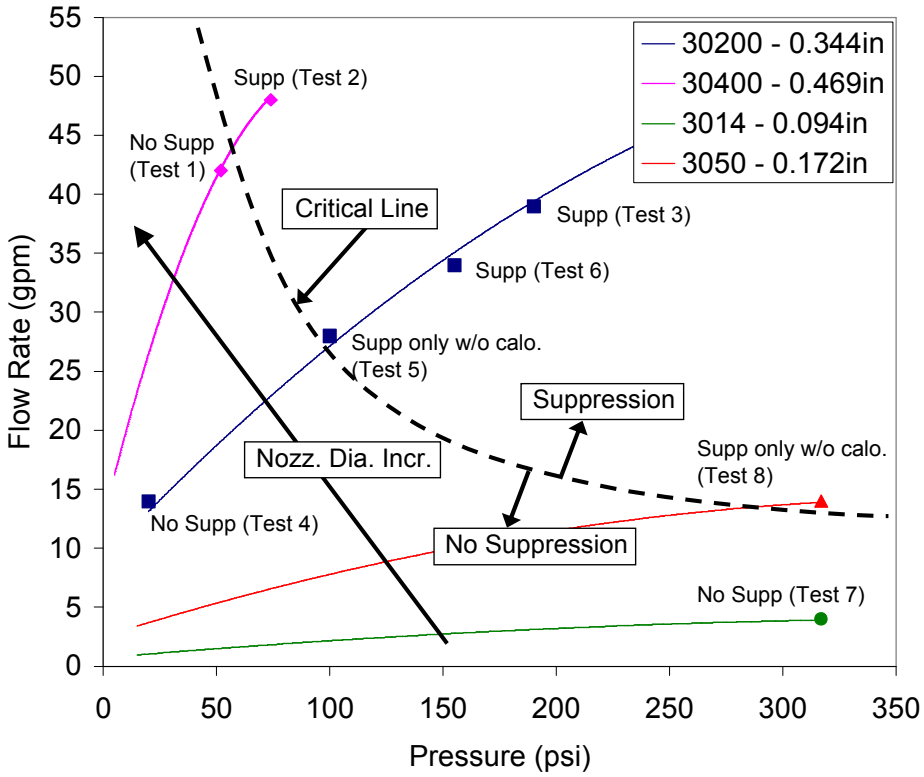


**Fig. 5. Critical Line for Suppression for 90° Spray Injection.**

Suppression was achieved when the operating flow rates and pressures were on the high end of the nozzle operating curve. For example, in the case of nozzle 30200 (0.344 in nozzle diameter), suppression was not achieved with and without the calorimeter when the flow rate was 14 gpm (see Test 4). For the same nozzle, suppression was achieved without the calorimeter when the flow rate was 28 gpm (Test 5). Finally, for the same nozzle, suppression was achieved with and without calorimeter at greater flow rates (Test 6 and Test 3). Similar trends were observed with nozzle 30400 (0.469 in nozzle diameter), although at different operating conditions and in only two tests. In the case of nozzle 3050 (0.172 in nozzle diameter), suppression was achieved without the calorimeter at 14 gpm, the highest flow rate the suppression system could operate with this nozzle. For nozzle 3014 (0.094 in nozzle diameter), suppression was not achieved at all regardless of the presence of the calorimeter.

For the 45° nozzles experiments, suppression was consistently achieved only with nozzle pressure at 190 psi and only without the calorimeter. No suppression occurred at the lower

pressures and results were not repeatable at the mid- to upper range of operating pressure. In the case at 190 psi without the calorimeter, the suppression time reached nearly 10 times the suppression time of the 90° injection angle experiments. The reason for the poor performance of the 45° nozzle configuration is attributed to the several factors; the spray travel distance was relatively long and the spray was unevenly distributed across the fire, stirring the fire and enhancing the mixing rate. Note also that objects in the flame zone can adversely affect the suppressant flow; recirculation zones that form on the downstream sides of objects have been identified as favorable for flame stabilization [5]. Of the various stabilized fires, liquid pool fires established behind obstructions have been identified as some of the most challenging to suppress.

## SUPPRESSION MODELING

### Two Phase Flow Modeling

Numerical simulations are conducted using Sandia's fire field modeling code. VULCAN. The Eulerian gas phase is solved assuming the Temporally Filtered Navier-Stokes (TFNS) turbulence closure model [2]. The "Eddy Dissipation Concept" (EDC) combustion model of Ertesvag and Magnussen [3] is used to model turbulent combustion as extended by Tieszen and Black [4] and Hewson et al [5] to include the effects of flame suppression. Details of the flame suppression will be given in the next section. Soot formation and absorption properties are based on the work of Tesner [6], and a discrete transfer method is used to solve for the radiation heat transfer. The gas-phase flow is calculated on an Eulerian staggered Cartesian grid using the pressure correction method of the SIMPLE algorithm [7]. A second-order up-winding and centered scheme is used for the convective and diffusion terms, respectively, in solving the transport differential equations.

The water spray model is based on a Lagrangian stochastic separated flow approach [8, 9]. Evolution equations for collections of droplets with similar sizes and initial conditions, denoted as parcels, are used to reduce the computational cost. The parcels are advanced under the influence of modeled turbulent fluctuations in the gas-phase properties. Maxey and Riley's [10] momentum equation for a small rigid sphere in a non-uniform flow is used. Evaporation is modeled using a thin skin model with standard convective correlations for heat and mass transfer. Droplet-droplet collisions are modeled using the model of Ko et al [11]. This approach only accounts for either droplet-droplet 'bouncing' or 'coalescence', and not a droplet-droplet 'shattering' effect that produces additional drops. The 'shattering' effect may become important for the head-to-head colliding sprays [12]. Since all droplets are typically moving in the same direction in our spray, the "shattering" is unlikely to occur. Droplet breakup due to aerodynamic forces is modeled using the Taylor Analogy Breakup (TAB) Model of O'Rourke and Amsden [13].

Particle turbulence interaction models are introduced at the parcel and sub-parcel level to account for the effect of local fluctuations in the velocity field while the rest of the thermo-physical variables are approximated by their corresponding time averaged values. The velocity-fluctuation models serve to increase the droplet dispersion, mimicking the effects of unresolved turbulent eddies. These unresolved turbulent motions are significant for the present high-pressure sprays that generate substantial turbulent kinetic energy. The parcel turbulence model accounts

for the effects of turbulent eddies perturbing the parcel trajectory and is based on the random walk model of Gosman and Ioannides [14], as modified by Shuen et al [15]. Within a parcel, the spatial distribution of particles is assumed to be of Gaussian form. The standard deviation of this spatial distribution evolves with time for each parcel as discussed by Zhou and Yao [16].

The VULCAN suppression model is based on the concept of a critical Damkohler number for extinction where the Damkohler number represents the ratio between the chemical and fluid mixing time scales. This captures the physics of both oxygen depletion and cooling of the flame in fire suppression because both act to increase the chemical time scales. The chemical time scales are determined by conducting a series of computations of the blow-out limits for a perfectly-stirred reactor (PSR). Further details on suppression model are available in Ref. [1, 8].

## Computational Details

The water spray was injected directly above the pool fire center at a height of 5 m, and the droplet velocity was varied from 20 m/s to 60 m/s. The time step used for the gas-phase simulation was allowed to vary between 0.01 sec and 0.0001 sec to maintain a peak Courant number of 0.5 and below. The sub-cycling time step for the liquid phase was approximately $\Delta t_{liq} \approx \Delta t_{gas} / 100 \sec$ , set by the stability criterion implemented in the fire suppression code with the given maximum injection speed. The grid was stretched to provide fine resolution near the pool fire, for a computational node count of 168,116 (or 53 x 52 x 61). The cone angle of the spray was set at 30° and the spray injection was initiated at t=5 sec. The total number of computational parcels injected was 50,000 parcels during a 5 sec spray injection duration (or 10,000 parcels/sec). The total number of water droplets ranged from 13.1 x $10^6$ to 1.1 x $10^9$. This yielded 260 to 22,000 droplets per parcel. Each parcel contains a comparable mass of water (parcels with smaller particles contain more particles). The initial droplet size distribution was assumed to be the Rosin-Rammler distribution shape (i.e., $PDF(D) = \left(qD^{q-1} / X^q\right)\exp\left(-\left(D/X\right)^q\right)$, where $D$ is the droplet diameter and $X$ is the characteristic or mean droplet size) with the corresponding dispersion coefficient of $q$ = 1.8, deduced from the measurement of a typical commercial nozzle obtained from Spray System Co., IL.

## JP8 Pool Fire Predictions

Figure 6a (no water spray) shows the local gas temperature at various physical heights; a quasi-steady state is reached at about t~5 sec. It is also evident that the higher locations have the higher gas temperature. As the height increases, the temperature fluctuations increased due to flame fluttering at its top. Puffing also launches wave generation from the pool's bottom, which in turn renders severe wave propagation (or fluttering) at the flame top.

## Test 3: High Injection Pressure

Test 3 was simulated using the operating conditions for the nozzle model no. 30200: the nozzle diameter was 0.344", the operating pressure was 190 psi, the mass flow rate was 2.46 kg/s, and the average mean diameter and the dispersion coefficient of the Rosin-Rammler distribution were 370 μm and 1.8, respectively. Due to its relatively high injection pressure, the initial droplet

size at the nozzle exit was relatively small. A high evaporation rate produced a rapid cooling of both the flame and the surface of the pool.

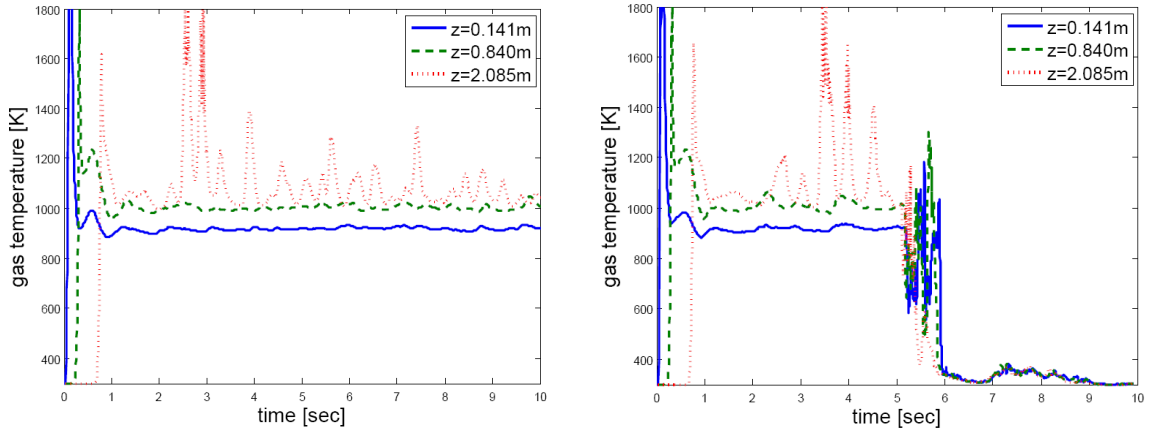


(a) A quasi-steady state (b) Test 3

**Fig. 6. Time histories of the centerline local gas temperature at various heights.**

Upon spray injection at 5 s, the flame shape is changed due to the spray momentum projection toward the flame. The spray momentum is large enough to overcome the rising buoyancy force of the flame. As a result, soon after the initiation of the water spray (t=5.9 s), the flame column quickly disappears and flattens near the pool surface. At about t=7 s, the fire is strongly suppressed. A small flame still survives at the pool's edge which causes an increase in the gas temperature at t=7 s, as shown in Figure 6b. The fire is eventually fully extinguished, finally reaching 300 K gas temperatures for all locations.

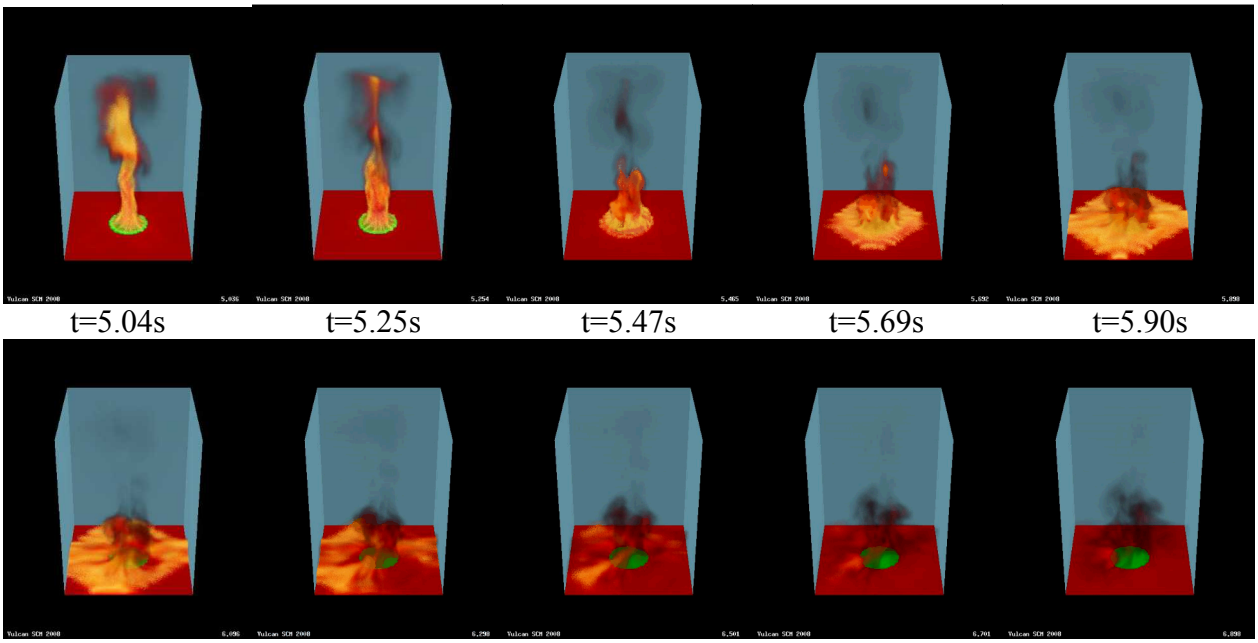


**Fig. 7. Vulcan fire suppression code result for Test 3. Suppression was achieved within 2 seconds, from the point of water spray injection (5 sec) to about 7.0 sec.**

Figure 6b shows gas temperature spikes observed after the initiation of water spray at about 5.6 s and at relatively low heights. Because the water spray nozzle is located at 5 m above the pool, the gas in the proximity of the nozzle experiences cooling of the water spray first, while lower parts of the flame undergo enhanced combustion. The enhanced combustion is presumably due to the entrainment of air with the spray and the increased momentum that enhances turbulent fuel-air mixing. This explanation is consistent with the qualitative volume-rendered temperature results of the simulations shown in Figure 7.

The enhanced mixing due to spray injection is also seen in the experiment in Figure 4. The fire plume is at its maximum size about one second after the water spray injection (t~6 s). The fire appears to be completely suppressed at the pool's surface at t>6.33 s (though it is possible a few flames may still remain at the pool). Lingering flames observed in the model prediction in Figure 7 did not seem to occur in experiment. In Figure 4, a lifted flame continues to rise at about 1.3 s after spray initiation and eventually dissipates.

**Test 4: Low Injection Pressure**

Test 4 was simulated with the following initial conditions: nozzle model no. 30200, nozzle diameter d=0.344", an injection pressure of 25 psi, a mass flow rate of 0.883 kg/s, and the average mean diameter was 870 μm and the dispersion coefficient of the Rosin-Rammler distribution $q$ was 1.8. Due to the relatively low injection pressure the initial droplet size at the nozzle exit was relatively large. Figure 8 shows temporal changes of the gas temperature for Test 4 at various heights.

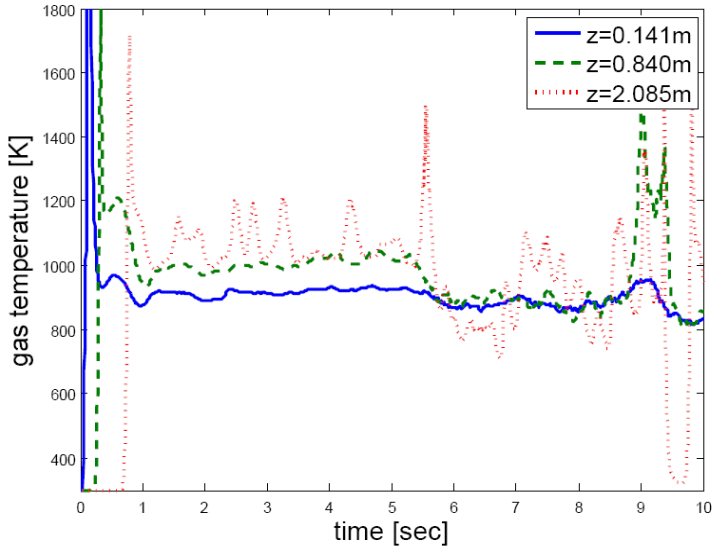


**Fig. 8. Time histories of gas temperature at the pool fire center for Test 4.**

Flame extinction was not achieved in the simulation of Test 4 though the flame does recognize the presence of the water spray as suggested by the variations in temperatures from the baseline fire case. The flame's buoyancy force is strong enough or the spray momentum is too weak to

significantly change the morphology of the flames, as indicated in Figure 9. This computational result is consistent with the observed experimental results.

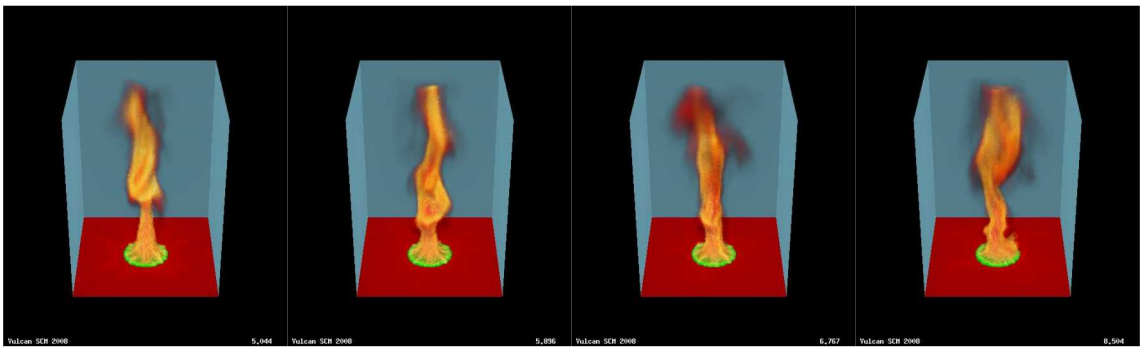


**Fig. 9. Vulcan fire suppression code result for Test 4. Suppression was *not* achieved from injection start (t=5 sec) to the end of the simulation (t=10 sec).**

## CONCLUSIONS

A series of water spray fire suppression benchmark tests were performed. Boundary conditions and temporal data were measured to support model development and validation efforts for the evaluation of the SNL VULCAN fire physics code. A total of twelve test configurations were conducted. Test parameters include nozzle size, orientation, operating pressure, and the presence (or not) of a large object inside the fire. Results of the 90° and the 45° spray orientations were significantly different. Results of 90° showed the suppression was achieved above a critical line. Operating in a regime below the critical line will not yield a complete suppression condition (i.e., extinguishment) and any operating regime above the line will guarantee extinguishment for the case without the calorimeter. For the 45° spray angle suppression tests, the fire extinguishment was consistently achieved only when the operating pressure was greater than 190 psi and only for the test cases without the calorimeter. Since test data for the 45° spray angle configuration were not repeatable, these data are not recommended for model validation. Limited simulations of the benchmark tests produced results consistent with the experimental observations.

### Acknowledgements

This study was sponsored by the Department of Defense (DTRA) and was performed at Sandia National Laboratories. This work was supported by the United States Department of Energy and was performed at Sandia National Laboratories. Sandia is a multiprogram laboratory operated by Sandia Corporation, a Lockheed Martin Company, for the United States Department of Energy under Contract No. DE-AC04-94AL85000.

## REFERENCES


[1] S.J. Yoon, H.Y. Kim, P.E. DesJardin, J.C. Hewson, S.R. Tieszen, T.K. Blanchat, "Unsteady RANS Modeling of Water-Spray Suppression for Large-Scale Compartment Pool Fires," *Atomization and Sprays*, Vol. 17, Issue 1 (2007).

[2] S.R. Tieszen, S.P. Domino, A.R. Black, "Validation of a Simple Turbulence Model Suitable for Closure of Temporally-Filtered Navier-Stokes Equations Using a Helium Plume," Sandia National Laboratories Report SAND 2005-3210 (2005).

[3] S. Ertesvag, B.F. Magnussen, "The Eddy Dissipation Turbulence Energy Cascade Model," *Combustion Science and Technology*, 159:213-235 (2000).

[4] S.R. Tieszen, A.R. Black, "Development of a Subgrid Fire Extinguishment Model," Sandia National Laboratories Report SAND2001-3321 (2001).

[5] J.C Hewson, S.R. Tieszen, W.D. Sundberg, P.E. DesJardin, "CFD Modeling of Fire Suppression and its Role in Optimizing Suppressant Distribution, *Proc. of the 2003 Halon Options Tech. Working Conf.*, Albuquerque, NM (2003).

[6] P.A. Tesner, "Growth Rate of Soot Particles," *Combustion Science and Technology*, 97:243-245 (1994).

[7] S.V. Patankar, Numerical Heat Transfer and Fluid Flow, Taylor & Francis, Editor (1980).

[8] P.E. DesJardin, L.A. Gritzo, "A Dilute Spray Model for Fire Simulations: Formulation, Usage and Benchmark Problems, Sandia National Laboratories Report SAND2002-3419 (2002).

[9] S.J. Yoon, J.C. Hewson, P.E. DesJardin, D.J. Glaze, A.R. Black, R.R. Skaggs, "Numerical Modeling and Experimental Measurements of a High Speed Solid-Cone Water Spray for Use in Fire Suppression Applications," *Int. Jr. Multiphase Flow*, 30:1369-1388 (2004).

[10] M.R. Maxey, J.J. Riley, "Equation of motion for a small rigid sphere in a non-uniform flow. *Physics of Fluids*, 26:883-889 (1983).

[11] G.H. Ko, S.H. Lee, H.S. Ryou, Y.K. Choi, "Development and Assessment of a Hybrid Droplet Collision Model for Two Impinging Sprays. *Atomization and Sprays*, 13:251-272 (2003)

[12] T.L.Georjon, R.D. Reitz, "A Drop-Shattering Collision Model for Multidimensional Spray Computations," *Atomization and Spra*ys, 9:231-254 (1999).

[13] P.J. O'Rourke, A.A. Amsden, "The TAB Method for Numerical Calculation of Spray Droplet Breakup, SAE Technical Paper 872089 (1987).

[14] A.D. Gosman, E. Ioannides, E., "Aspects of Computer Simulation of Liquid-Fueled Combustion," *19th AIAA Aerosp. Sci. Meeting*, St. Louis, MO, AIAA-81-0323 (1981).

[15] J.S. Shuen, L.D. Chen, G.M. Faeth, "Evaluation of a Stochastic Model of Particle Dispersion in a Turbulent Round Jet," *AIChE Journal*, 29:167-170 (1983).

[16] A. Zhou, S.C. Yao, "Group Modeling of Impacting Spray Dynamics, *Int. Journal of Heat Mass Trans.* 35:121-129 (1992).